INORGANIC CHEMISTRY
FRONTIERS

REVIEW

View Article Online
View Journal | View Issue

Cite this: *Inorg. Chem. Front.*, 2021, **8**, 2634

Heterometallic coordination polymers as heterogeneous electrocatalysts

Naoto Kuwamura and Takumi Konno *

Heterometallic coordination polymers are emerging as a class of crystalline materials for sustainable energy production *via* electrocatalysis, thanks to the synergistic and cooperative effects of different kinds of metal centres present in these polymers. The development of this class of materials mainly relies on screening experiments using a one-pot protocol of mixing metal ions; notably, the incorporation of different metal ions into desired positions in a single polymeric structure is quite difficult. This review article briefly summarizes the synthesis methods for heterometallic coordination polymers that show heterogeneous electrocatalytic activity. In addition, the relationships between the molecular structure and hydrogen evolution (water/proton reduction), oxygen evolution (water oxidation), CO_2 reduction, oxygen reduction, and some important organic reactions are reviewed to offer new ideas for designing efficient energy conversion materials and developing new classes of heterometallic coordination polymers.

Received 27th January 2021,
Accepted 9th March 2021

DOI: 10.1039/d1qi00112d

rsc.li/frontiers-inorganic

1. Introduction

Coordination polymers (CPs) are crystalline solids with infinite structures that are sustained by coordination bonds between metal ions or metal clusters and organic linker molecules, including metal–organic frameworks (MOFs) as a CP subclass.[1] Since the definition of CPs in 1964,[2] this class of compounds has continuously been a hot research topic due to not only their diverse structural aspects but also their wide range of applications, such as sensors,[3,4] gas storage materials,[5,6] magnets,[7,8] and catalysts.[9,10] One of the important characteristics of CPs is their crystallinity, which allows X-ray crystallography to be used to determine their structures at an atomic level. To date, a large variety of compositions and structures of CPs have been designed and synthesized using various organic ligands, metal ions, synthesis conditions, protocols, and in

Department of Chemistry, Graduate School of Science, Osaka University, Toyonaka, Osaka 560-0043, Japan. E-mail: konno@chem.sci.osaka-u.ac.jp

Naoto Kuwamura

Naoto Kuwamura received his B.S., M.S. and Ph.D. degrees from Osaka City University in 2006, 2008 and 2011, respectively. He then successively moved to the Max-Planck Institute of Bioinorganic Chemistry (currently, Max-Planck Institute for Chemical Energy Conversion) as a postdoctoral research fellow. In 2012, he moved to Osaka University where he is currently an assistant professor. His research interest is directed toward the creation and voltammetric analysis of heterometallic multinuclear complexes based on thiolate ligands that show unique redox properties in both solution and solid states.

Takumi Konno

Takumi Konno received his Ph.D. degree from the University of Tsukuba in 1985. He continued his work there before moving to the University of Cincinnati in 1986. He became an assistant professor at the University of Tsukuba in 1987 and was promoted to a lecturer in 1994. In 1997, he moved to Gunma University as an associate professor and was promoted to a full professor in 1998. He was appointed as a professor at Osaka University in 2000. His research interests are currently focused on creating a new class of functional multinuclear and metallosupramolecular coordination compounds based on metal complexes with simple thiolate ligands.

some cases, post-synthesis treatments. In addition, studies on the relationships between the structures of CPs and their functionalities have been conducted to develop desirable functions,[11] which have been summarized in recent review articles.[12]

CPs can be classified into homometallic (one kind of metal ion) and heterometallic (more than two kinds of metal ions) species. Recently, growing interest has been directed towards heterometallic CPs because the presence of different kinds of metal ions in one structure often provides synergistic and cooperative effects on their functionalities; notably, these effects are not realized in homometallic CPs.[13–17] For example, heterometallic CPs have been increasingly studied as a new class of heterogeneous catalysts for photochemical reactions[18] and organic reactions[19] due to their uniform arrangement of redox/catalytically active sites in their network structures. The availability of CPs as heterogeneous electrocatalysts is also a recent hot topic[20] because electrocatalysis is an energy-related technology that can contribute to the future development of sustainable energy-related reactions, such as hydrogen evolution, oxygen evolution, oxygen reduction, CO_2 reduction, and organic transformation. However, in most cases, CPs have been used as precursors to obtain inorganic composite materials by annealing at high temperature, which results in the complete decomposition of their original frameworks.[21–24] Thus, studies on the use of CPs themselves as electrocatalysts are needed to realize cost-effective and energy-efficient electrocatalytic reactions.

In this review article, we summarize heterometallic CPs that have been applied as heterogeneous electrocatalysts. First, the synthesis approaches for incorporating two or more kinds of metal ions into a single polymeric structure are summarized. The incorporation of several kinds of metal ions in a single CP structure has commonly been achieved by one-pot reactions in which different kinds of metal ions with different coordination properties are mixed with organic ligands.[25] Another method to achieve this, so-called metalloligand approach, is the use of isolated metal complexes that possess donor site(s) for binding metal ions to form heterometallic multinuclear structures.[26] Following the first section, the relevance of the structural aspects of CPs, such as their dimensionalities, combinations of metal ions, coordination environments, and porosities, to their electrocatalytic activities is described, together with representative examples. Closely related review articles that summarize MOF-based electrocatalysts have appeared previously.[27–29] Very recently, heterotrimetallic MOFs that show electrocatalytic oxygen evolution have also been reviewed.[30,31] This review article focuses on summarizing the synthesis methodologies of heterometallic CPs and their utility for their various 'heterogeneous' electrocatalytic activities from the viewpoint of coordination chemistry.

2. Synthesis methods for heterometallic coordination polymers

Conventionally, CPs have been produced by simple mixing of organic ligands and metal ions in a one-pot manner.[32] On the other hand, the synthesis situation of heterometallic CPs is different, and three synthesis techniques have been applied to incorporate two or more kinds of metal ions into polymer structures (Fig. 1): (i) a self-assembly method (or one-pot synthesis), (ii) a metalloligand approach,[33] and (iii) post-synthesis modification.[34]

The simplest and most popular synthesis approach is the conventional (i) self-assembly method, where several kinds of metal ions are mixed with organic and/or inorganic ligands under specific conditions, and a large number of heterometallic CPs have been produced by this method so far.[35] While this approach does not involve the pre-treatment of starting materials, different kinds of metal ions with similar characteristics, such as ionic radius, charge, and Lewis acidity, normally need to be selected for this synthesis approach. In addition, CPs synthesized by this approach are often produced as non-crystalline solids,[36] which prevents the determination of their structures at an atomic level by X-ray crystallography. Therefore, the limitations of employed metal ions and the difficulty in structural determination are serious problems in producing CPs by the self-assembly method.

An alternative synthesis method that has recently attracted the attention of researchers is (ii) the metalloligand approach.[37] In this approach, metal complexes bearing donor site(s) are used as a 'metalloligand', which reacts with target metal ions to form heterometallic CPs. This method allows for the control of the structures and dimensionalities of CPs *via* the proper choice of metalloligands and target metal ions, which act as the nodes and linkers in the produced polymeric

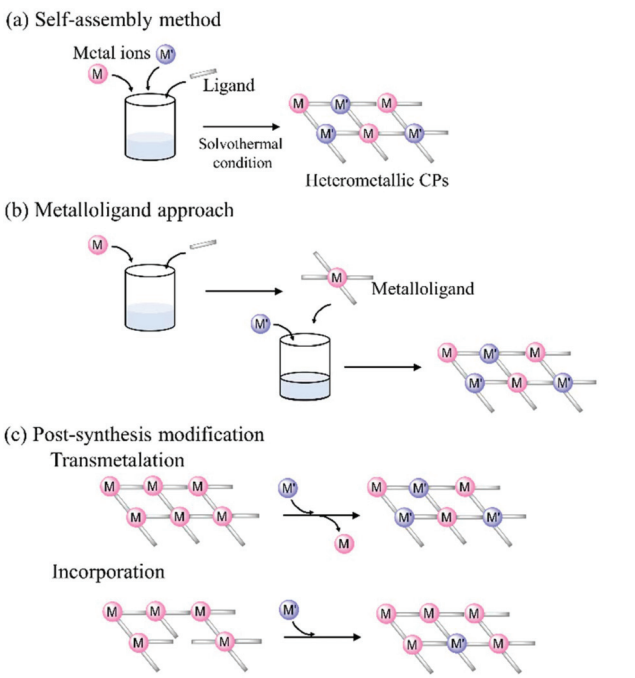

Fig. 1 General synthesis methods for heterometallic coordination polymers: (a) self-assembly method, (b) metalloligand approach, and (c) post-synthesis modification.

structures, respectively. For the synthesis of heterometallic CPs that show electrocatalytic activities, redox-active metalloligands bearing open metal site(s) are used,[38] and the design and preparation of metalloligands are important for this synthesis approach.

To synthesize heterometallic CPs that show electrocatalytic activities, (iii) a post-synthesis modification, in which catalytically active guest species are incorporated into the framework of a pre-synthesized CP, has also been employed.[39] In this approach, guest species are designed to interact with the framework of CPs and to migrate into the pores of CPs. The exchange of metal ions in CPs by catalytically active metal ions is also useful to produce electrocatalytic CPs.[40] In general, this approach is applicable for CPs having inherently labile metal ions such as Ni^{II}, Zn^{II}, and Cd^{II}, which can be replaced by external metal ions.

For heterometallic CPs that show electrocatalytic activities, the important structural factors are a (i) redox centre (metal ion) with one or more vacant coordination site(s), (ii) mass transport space and/or channel, (iii) conductive linkage, and (iv) stable framework structure.[41] A short distance between the metal centres is also important for electronic communication between the catalytic centres in heterometallic CPs.[42–44] In some cases, additives such as metal clusters (redox centre), Nafion (ion-conductive material or binder), and activated carbon (electrically conductive material) are incorporated to endow heterometallic CPs with electrocatalytic activity. Currently, optimizing the electrode fabrication method makes it possible to investigate the redox behaviour of heterometallic CPs that are insoluble in any solvents without decomposition.[45–47]

3. H_2 evolution electrocatalysis

Hydrogen gas (H_2) is a clean and renewable energy source that is an alternative to fossil fuels because H_2 produces only water when reacted with O_2. To generate this renewable energy source, water (or proton) reduction catalysts are in high demand.[48] In the past few decades, coordination chemistry has widely contributed to the research field of electrocatalysts for water reduction based on the synthesis of new coordination compounds.[49] Early works on the hydrogen evolution system started from Prussian white which was homometallic Fe^{II} CP.[50,51] Note that it is easy to incorporate two kinds of metal ions into Prussian blue analogues by mixing hexacyanido complexes and metal ions in a self-assembly method because many types of hexacyanido complexes with different metal centres have been discovered.[52] Abe *et al.* demonstrated that the integration of Fe^{III} and Ru^{II} in a Prussian blue analogue leads to enhanced hydrogen evolution activity with a turnover frequency (TOF) of 2.5×10^2 s^{-1} at an onset potential of −0.6 V (*vs.* Ag/AgCl).[53,54] Other combinations using Ni^{II}, Co^{II}, Pb^{II}, Cu^{II}, Mn^{II}, and Zn^{II} as the metal components of Prussian white analogues also exhibit appreciable electrocatalytic activities for hydrogen evolution.[55]

Polyoxometalates (POMs) are inorganic cluster species that generally comprise early transition metals such as W, Mo, and V.[56] This class of compounds is the most popular heterometallic electrocatalyst for H_2 evolution because it is easy to integrate different kinds of metal ions into a POM framework.[57] While homometallic POMs are generally unstable in non-acidic solution, several heterometallic POMs can be handled in neutral water, which allows them to be used as building blocks for the preparation of POM-based CPs.[58] It has been reported that a Zn^{II}–Mo^{V}-POM-based CP exhibits hydrogen evolution activity at pH 1, showing a Tafel slope of 96 mV deg^{-1} with an overpotential of 180 mV.[59] Ma *et al.* reported a Cu^{II}-MOF that contains W^{VI}-POM molecules.[60] The incorporation of W^{VI}-POM molecules into the MOF provided high chemical stability, allowing the material to exhibit electrocatalytic activity for H_2 evolution at a low overpotential of 131 mV with a Tafel slope of 51 mV deg^{-1}. The exchange of countercations in anionic POMs by metal complexes is also an effective way to obtain heterometallic CPs consisting of POM molecules.[61] Gomez-Mingot *et al.* studied the inclusion effect of complex cations on framework structures and electrocatalytic activities using anionic Zn^{II}–Mo^{V}–Mo^{VI}-POMs as a host compound.[62] The inclusion of cationic species strongly affected the catalytic hydrogen evolution activity, resulting in a TOF of 9.3×10^{-2} s^{-1} with an overpotential of 419 mV.[62]

As part of our study on the creation of heterometallic CPs based on S-donating metalloligands with D-penicillaminate (D-pen),[63–65] we recently discovered (in 2017) the first example of a heterotrimetallic coordination polymer that showed heterogeneous catalytic activity for hydrogen evolution under electrochemical conditions.[66] In this study, we employed a Pt^{II} metalloligand with D-pen,[67] which reacted stepwise with Pd^{II} and Ni^{II} ions to produce a heterotrimetallic CP containing all three group 10 metal ions. In this compound, $Pt^{II}_2Pd^{II}_2$ tetranuclear units were linked by Ni^{II} ions through D-pen carboxylate groups in a 1D chain structure.[66] The combination of the Pt^{II} metalloligand with Pd^{II} and Ni^{II} in the $(Pt^{II}_2Pd^{II}_2Ni^{II})_n$ coordination polymer significantly enhanced heterogeneous catalytic activity for electrochemical hydrogen evolution, showing a TOF of 0.011 s^{-1} at an onset potential of −0.98 V (*vs.* Ag/AgCl). More recently, we prepared 2D and 3D $(Pt^{II}_2Pd^{II}_2Mn^{II}_2)_n$ heterotrimetallic CPs by using Mn^{II} instead of Ni^{II} as linker ions, the dimensionality of which was controlled by counteranions (Cl *vs.* Br).[68] The 2D and 3D $(Pt^{II}_2Pd^{II}_2Mn^{II}_2)_n$ CPs showed activities much higher than the 1D $(Pt^{II}_2Pd^{II}_2Ni^{II})_n$ CP, which was explained by the stronger Lewis acidity of the active centres of Pd^{II} in the $Pt^{II}_2Pd^{II}_2$ units and an increase in framework robustness due to their higher dimensionalities. Budnikova's group developed ferrocene-based metalloligands that coordinated to 3d metal ions to form 1D heterobimetallic CPs.[69] Due to the presence of ferrocenyl units, the heterobimetallic CPs were redox active. This coordination contributed to a higher electrocatalytic activity for H_2 evolution, showing Tafel slopes of 120 mV deg^{-1} and 110 mV deg^{-1} at overpotentials of 450 mV and 340 mV for the heterobimetallic CPs with Co^{II} and Zn^{II}, respectively. Additionally, these 1D heterobimetallic CPs have

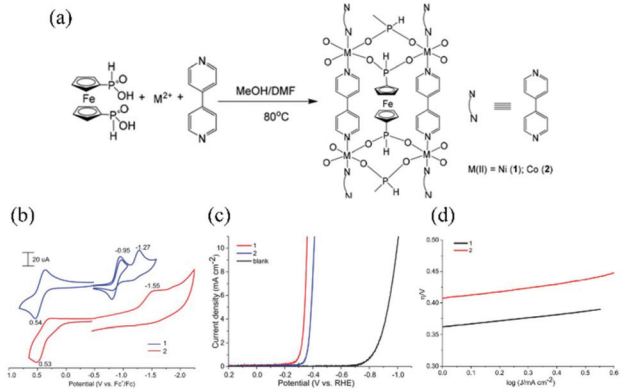

Fig. 2 Co^{II}/Ni^{II}–Fe^{II} bimetallic coordination polymers as a H_2 evolution electrocatalyst: (a) synthesis scheme, (b) CV curves in MeCN containing 0.1 M $^tBu_4NBF_4$ with a sample-modified glassy carbon electrode, (c) LSV curves in 0.5 M H_2SO_4 at a scan rate of 0.05 V s^{-1}, and (d) their corresponding Tafel plots. Adapted from ref. 70 with permission from The Royal Society of Chemistry.

been extended to higher-dimensional CPs by the addition of 4,4′-bipydine ligands (Fig. 2).[70] The CPs with Ni^{II} and Co^{II} showed Tafel slopes of 60 mV deg^{-1} and 65 mV deg^{-1} at overpotentials of 350 mV and 400 mV, respectively, which is the best performance for 4,4′-bipydine-incorporated CPs. A combination of high electrical conductivity and the presence of exposed catalytically active centres is important in MOFs to act as excellent heterogeneous electrocatalysts. Indeed, Zhang and Chen *et al.* demonstrated that Ni^{II}–Co^{II} and Ni^{II}–Cu^{II} 2D MOFs containing a π-conjugated organic ligand (hexaiminohexaazatrinaphthalene) showed high electrocatalytic activity;[71] the electrocatalytic performance for H_2 evolution was evaluated by Tafel slopes of 98.2 mV deg^{-1} and 101.5 mV deg^{-1} with overpotentials of 207 mV and 162 mV for Ni^{II}–Co^{II} and Ni^{II}–Cu^{II} MOFs, respectively. Farha and Hupp *et al.* reported a Zr^{IV}-based MOF that was functionalized with MoS_x catalytic units,[72] which exhibited high electrocatalytic activity for H_2 evolution. This compound was prepared *via* the post-synthesis method, with a Zr^{IV}-based MOF being reacted with Mo^{VI} species in the presence of H_2S gas. The presence of large pores in the crystal lattice of the precursor MOF, together with the high stability of its framework towards chemical stimuli, allowed the application of the post-synthesis method. Other examples of heterometallic CPs that act as heterogeneous electrocatalysts for H_2 evolution are summarized in Table 1.

4. O_2 evolution electrocatalysis

While oxygen (O_2) evolution is an important anodic half reaction of water splitting and is paired with cathodic hydrogen (H_2) evolution, its reaction suffers from sluggish kinetics because of the requirement of four electrons and four protons for O–O bond formation.[73] Thus, efficient electrocatalysts must be developed to overcome the kinetic barrier of O_2 formation.[74] To date, considerable efforts have been devoted to investigating molecular electrocatalysts for O_2 evolution by using discrete metal complexes and homometallic CPs.[75] An early work on O_2-evolving electrocatalysts based on heterometallic CPs used Prussian blue analogues.[76] A film of a Co^{II}–Fe^{II} Prussian blue analogue was attached on an electrode by electrochemical deposition and water oxidation was performed to produce O_2 gas with a TOF of 0.5 s^{-1} at an overpotential of 550 mV. The electrocatalytic activity of this compound is due to its open channel structure for mass transport and electron conductivity and the presence of catalytically active Co^{II} centres. The Karadas group employed Prussian blue analogues with other combinations of metal ions, such as Co^{II}–Co^{III}, Co^{II}–Cr^{III}, Co^{II}–Fe^{II}, and Co^{II}–Fe^{III}, to investigate the effect of metal ions co-existing with Co^{II} ions in the Prussian blue framework on their electrocatalytic activities for water oxidation (Fig. 3).[77] They showed that the electron density of the catalytic centre of Co^{II} was affected by the co-existing metal ions, which was strongly related to their electrocatalytic activities. The catalytic activities of Prussian blue analogues are not high because their catalytically active sites (related to the so-called surface concentration) are not well exposed; all the metal centres have an octahedral geometry and are coordinated by six cyanide ligands, except for the terminal metal ions of the network structure. To increase catalytic activity, the Karadas group incorporated a pyridyl-based polymer, poly(4-vinylpyridine), into Prussian blue analogues,[78] which resulted in the production of amorphous solids with high surface concentrations and low overpotentials. A Ni^{II}–Fe^{III} bimetallic CP with phthalocyanine ligands also acts as a heterogeneous electrocatalyst for water oxidation.[79] In this case, both the Ni^{II} and Fe^{III} ions are assumed to be catalytic centres in the 2D sheet structure. The catalytic activity of the Ni^{II}–Fe^{III} CP is higher than the activities of the corresponding Ni^{II} and Fe^{III} homometallic CPs, indicating the positive synergistic effect of the two kinds of metal centres on catalysing the water oxidation reaction.

Recently, our group reported the catalytic behaviour of Pt^{II}–Cu^{II}–Zn^{II} heterotrimetallic CPs with perchlorate or chloride counteranions for water oxidation; these compounds were synthesized *via* the metalloligand approach using a Pt^{II} metalloligand with D-pen (Fig. 4).[80] In these compounds, $Pt^{II}_2Cu^{II}_2$ tetranuclear units were linked by Zn^{II} ions through D-pen carboxylate groups in a polymeric structure. Notably, the CPs had different dimensional structures (2D *vs.* 3D) and different coordination geometries around Cu^{II} centres (square plane *vs.* octahedron) that were dependent on the counteranion (ClO_4^- *vs.* Cl^-). These differences largely influenced the heterogeneous electrocatalytic activity for water oxidation; the perchlorate salt with square-planar Cu^{II} centres showed a catalytic activity much higher than that of the chloride salt with octahedral Cu^{II} centres. While the electronic effect due to the coexistence of heterometallic ions remains unclear, this study revealed that the introduction of Cu^{II} ions into heterometallic CPs leads to heterogeneous electrocatalytic activity for water oxidation that is tuned by the linkage mode of Zn^{II} ions affecting the geometry of the Cu^{II} centres.

Table 1 Structural and electrocatalytic parameters for pristine H_2 evolution electrocatalysts based on their heterometallic coordination polymers

Compound	Dimension	Metal	Organic ligand/metalloligand	Onset potential	η	TOF	Tafel slope	Electrolyte	Ref.
Iron(III) ruthenocyanide	3D	Fe^{III} and Ru^{II}	CN^-	−0.6 V (*vs.* Ag/AgCl)	—	2.5×10^2 s^{-1} [a]	—	HCl–KCl (pH 1.5)	54
$[Zn(fcdHp)]_n$	1D	Zn^{II} and Fe^{II}	1,1′-Ferrocenylenebis(*H*-phosphinate) (fcd*H*p)	−0.220 V (*vs.* RHE)	340 mV (@ 10 mA cm^{-2})	4.5×10^{-3} s^{-1}	110 mV dec^{-1}	0.5 M H_2SO_4	69
$[Co(fcdHp)]_n$	1D	Co^{II} and Fe^{II}	1,1′-Ferrocenylenebis(*H*-phosphinate) (fcd*H*p)	−0.300 V (*vs.* RHE)	450 mV (@ 10 mA cm^{-2})	1.5×10^{-3} s^{-1}	120 mV dec^{-1}	0.5 M H_2SO_4	69
$[Ni(fcdHp)(4,4'\text{-bpy})]_n$	3D	Ni^{II} and Fe^{II}	1,1′-Ferrocenylenebis(*H*-phosphinate) (fcd*H*p) and 4,4′-bipyridine (4,4′-bpy)	−0.270 V (*vs.* RHE)	350 mV (@ 10 mA cm^{-2})	2.1×10^{-3} s^{-1}	60 mV dec^{-1}	0.5 M H_2SO_4	70
$[Co(fcdHp)(4,4'\text{-bpy})]_n$	3D	Co^{II} and Fe^{II}	1,1′-Ferrocenylenebis(*H*-phosphinate) (fcd*H*p) and 4,4′-bipyridine (4,5′-bpy)	−0.320 V (*vs.* RHE)	400 mV (@ 10 mA cm^{-2})	2.8×10^{-4} s^{-1}	65 mV dec^{-1}	0.5 M H_2SO_4	70
$[Ni(H_2O)_4Pd_2Pt_2(NH_3)_4(\text{D-pen})_4]Cl_2$	1D	Pd^{II}, Pt^{II} and Ni^{II}	D-Penicillaminate (D-pen)	−0.98 V (*vs.* Ag/AgCl)	—	1.1×10^{-2} s^{-1}	—	0.1 K $LiClO_4$	64
$[Mn_2Cl_2(H_2O)_6Pd_2Pt_2(NH_3)_4(\text{D-pen})_4]Cl_2$	2D	Pd^{II}, Pt^{II} and Mn^{II}	D-Penicillaminate (D-pen)	−1.0 V (*vs.* Ag/AgCl)	—	1.7×10^{-2} s^{-1}	—	0.1 K $LiClO_4$	68
$[Mn_2(H_2O)_6Pd_2Pt_2(NH_3)_4(\text{D-pen})_4]Br_4$	3D	Pd^{II}, Pt^{II} and Mn^{II}	D-Penicillaminate (D-pen)	−1.0 V (*vs.* Ag/AgCl)	—	4.1×10^{-2} s^{-1}	—	0.1 K $LiClO_4$	68
MOF									
$[Ni_3\{Co_3(HAHATN)_2\}]$	2D	Ni^{II} and Co^{II}	Hexaiminohexaazatrinaphthalene (HAHATN)	—	207 mV (@ 10 mA cm^{-2})	—	98.2 mV dec^{-1}	0.1 M KOH	71
$[Ni_3\{Cu_3(HAHATN)_2\}]$	2D	Ni^{II} and Cu^{II}	Hexaiminohexaazatrinaphthalene (HAHATN)	—	162 mV (@ 10 mA cm^{-2})	—	101.5 mV dec^{-1}	0.1 M KOH	71
POM-based compounds									
$(Bu_4N)_3[PMo^V_8Mo^{VI}_4O_{36}(OH)_4Zn_4](BTB)_{4/3}$	3D	Zn^{II} and $Mo^{V/VI}$	1,3,5-Benzenetribenzoate (BTB)	−0.180 V (*vs.* RHE)	237 mV (@ 10 mA cm^{-2})	—	96 mV dec^{-1}	0.5 M H_2SO_4	59
$(Bu_4N)_3[PMo^V_8Mo^{VI}_4O_{37}(OH)_3Zn_4](BPT)$	3D	Zn^{II} and $Mo^{V/VI}$	[1,1′-Bipheynyl]-3,4′,5-tricarboxylate (BPT)	−0.304 V (*vs.* RHE)	392 mV (@ 10 mA cm^{-2})	—	137 mV dec^{-1}	0.5 M H_2SO_4	59
$[Co(bpy)_3][PMo^V_8Mo^{VI}_4O_{37}(OH)_3Zn_4](trim)Co(bpy)_2(H_2O)$	1D	Co^{II}, Zn^{II} and $Mo^{V/VI}$	2,2′-Bipyridine (bpy) and 1,3,5-benzenetricarboxylate (trim)	−0.41 V (*vs.* Ag/AgCl)	452 mV (@ 10 mA cm^{-2})	4.5×10^{-2} s^{-1} [a]	—	0.1 M H_2SO_4	62
$(Bu_4N)_4[PMo^V_8Mo^{VI}_4O_{37}(OH)_3Zn_4](BTB)_{4/3}\cdot 1.5(H_3BTB)$	3D	Zn^{II} and $Mo^{V/VI}$	1,3,5-Benzenetribenzoate (BTB)	−0.45 V (*vs.* Ag/AgCl)	576 mV (@ 10 mA cm^{-2})	9.3×10^{-2} s^{-1} [a]	—	0.1 M H_2SO_4	62
$(Bu_4N)_2[Co(bpy)_3][PMo^V_8Mo^{VI}_4O_{37}(OH)_3Zn_4](BTB)_{4/3}\cdot 1.5(H_3BTB)$	3D	Co^{II}, Zn^{II} and $Mo^{V/VI}$	2,2′-Bipyridine (bpy) and 1,3,5-benzenetribenzoate (BTB)	−0.31 V (*vs.* Ag/AgCl)	419 mV (@ 10 mA cm^{-2})	9.3×10^{-2} s^{-1} [a]	—	0.1 M H_2SO_4	62

Table 1 *(Contd.)*

Compound	Dimension	Metal	Organic ligand/metalloligand	Onset potential	η	TOF	Tafel slope	Electrolyte	Ref.
$[Ru(bpy)_3]_4[PMo^{V}{}_8Mo^{VI}{}_4O_{38}(OH)_2Zn_4]_2(trim)_2$	3D	Ru^{II}, Zn^{II} and $Mo^{V/VI}$	2,2′-Bipyridine (bpy) and 1,3,5-benzenetricarboxylate (trim)	−0.45 V (*vs.* Ag/AgCl)	617 mV (@ 10 mA cm^{-2})	6.8×10^{-2} s^{-1} [a]	—	0.1 M H_2SO_4	62
$[PPh_4]_6[PMo^{V}{}_8Mo^{VI}{}_4O_{37}(OH)_3Zn_4]_2(trim)_2$	3D	Zn^{II} and $Mo^{V/VI}$	1,3,5-Benzenetricarboxylate (trim)	−0.27 V (*vs.* Ag/AgCl)	335 mV (@ 10 mA cm^{-2})	3.9×10^{-1} s^{-1} [a]	—	0.1 M H_2SO_4	62
$[Ru(bpy)_3]_3[PMo^{V}{}_8Mo^{VI}{}_4O_{37}(OH)_3Zn_4Cl]_2(biphen)_2$	2D	Ru^{II}, Zn^{II} and $Mo^{V/VI}$	2,2′-Bipyridine (bpy) and 4,4′-biphenyldicarboxylate (biphen)	−0.26 V (*vs.* Ag/AgCl)	337 mV (@ 10 mA cm^{-2})	3.0×10^{-1} s^{-1} [a]	—	0.1 M H_2SO_4	62
$[Cu^{II}_6(pzta)_6(bpy)_3(P_2W_{18}O_{62})]$	1D	Cu^{II} and W^{VI}	2,2′-Bipyridine (bpy) and 5-(2-pyrazinyl) tetrazole (pzta)	−0.076 V (*vs.* RHE)	131 mV (@ 10 mA cm^{-2})	—	51 mV dec^{-1}	—	60
$[Cu^{II}_6(pzta)_6(bpy)_3(As_2W_{18}O_{62})]$	1D	Cu^{II} and W^{VI}	2,2′-Bipyridine (bpy) and 5-(2-pyrazinyl) tetrazole (pzta)	−0.101 V (*vs.* RHE)	192 mV (@ 10 mA cm^{-2})	—	79 mV dec^{-1}	—	60

[a] The value was estimated by us based on the experimental data in the literature.

Fig. 3 Co^{II}–M^{III} bimetallic Prussian blue analogues as O_2 evolution electrocatalysts: (a) CV curves in 50 mM KP_i electrolyte at pH 7 with a sample-modified, fluorine-doped tin oxide (FTO) electrode at a scan rate of 0.05 V s^{-1}, (b) their corresponding Tafel plots, and (c) DFT calculation results. Adapted from ref. 77 with permission from John Wiley and Sons.

Fig. 4 Pt^{II}–Cu^{II}–Zn^{II} trimetallic coordination polymers as O_2 evolution electrocatalysts: (a) synthesis schemes, (b) packing structures of (left) a Cl salt and (right) a ClO_4 salt, and (c) LSV curves in CH_3CN–H_2O containing 0.1 M KPF_6 with a sample-modified glassy carbon electrode at a scan rate of 0.01 V s^{-1}. Adapted from ref. 80 with permission from The Royal Society of Chemistry.

In heterometallic MOF systems, dinuclear or trinuclear heterometallic units bridged by carboxylate groups are normally designed as a cluster node.[81] This class of compounds has been synthesized by the self-assembly method or post-synthesis transformation. Li and Lan explored Fe^{II}–Fe^{III}, Co^{II}–Fe^{III}, Ni^{II}–Fe^{III}, and Zn^{II}–Fe^{III} MOFs having a tricarboxylate ligand, all of which showed electrocatalytic activity for oxygen evol-

ution.[82] These MOFs were synthesized by the reaction of the trinuclear MFe_2^{III} cluster, $[MFe_2(\mu_3\text{-}O)(CH_3COO)_6(H_2O)_3]$ (M = Fe^{II}, Co^{II}, Ni^{II}, Zn^{II}), with biphyenyl-3,4′,5-tricarboxylate under solvothermal conditions. In the MOFs, the trinuclear cluster units were linked by the tricarboxylate ligands in a 3D network structure. The electrocatalytic behaviour was studied by using a carbon cloth electrode attached to a mixture of MOF and acetylene black *via* the drop-casting method. The heterometallic MOFs exhibited a more negative potential and a higher current density in the linear sweep voltammograms (LSVs) compared with the homometallic Fe^{II}–Fe^{III} MOF, indicating that the heterometallic MOFs performed electrocatalysis faster. In particular, the Ni^{II}–Fe^{III} MOF displayed an overpotential of 365 mV, which was lower than those of other heterometallic MOFs (Co^{II}–Fe^{III}: 376 mV and Zn^{II}–Fe^{III}: 522 mV), a homometallic Fe^{II}–Fe^{III} MOF (555 mV), and commercial IrO_2 (390 mV). Another Ni^{II}–Fe^{III} MOF with a 2D sheet structure was reported by Chen and Zhao.[83] This MOF was grown on nickel foam *via* one-step chemical bath deposition, where nickel foam was mixed with 2,6-naphthalenedicarboxylate, nickel acetate, and iron(III) nitrate in water. This material showed an overpotential of 240 mV at 10 mA cm^{-2} and a TOF of 3.8 s^{-1}, which are greater than those of the corresponding homometallic MOF and IrO_2 catalysts. Other examples of heterometallic CPs that act as heterogeneous electrocatalysts for O_2 evolution are summarized in Table 2.

5. CO_2 reduction electrocatalysis

To realize a future carbon-neutral society, the electrochemical conversion of CO_2 into useful chemical species has been intensively investigated in the past decade.[84] A homometallic Cu^{II} MOF was first applied for electrocatalytic CO_2 reduction in 2012,[85] and then, an increasing number of MOFs have been studied for electrochemical CO_2 reduction. An early work on electrocatalytic CO_2 reduction using a heterometallic MOF was performed by Yaghi and Yang in 2015. They applied a Co^{II}–Al^{III} MOF containing 4,4′,4″,4‴-(porphyrin-5,10,15,20-tetrayl)tetrabenzoate as a linker ligand for electrocatalytic CO_2 reduction.[86] In this case, a homometallic Al-MOF was directly grown on the electrode by the self-assembly method under solvothermal conditions, and then, the Co^{II}–Al^{III} MOF electrocatalyst was prepared by the post-binding of Co^{II} to the empty sites of the porphyrin units; this catalyst exhibited >76% selective CO production with a turnover number (TON) of 1400 and a stability of 7 hours. Kubiak *et al.* reported a Zr^{IV} MOF with Fe^{III} porphyrin units as a CO_2 reduction electrocatalyst, where the Fe^{III} porphyrin unit acted as a catalytic site in the Zr^{IV} MOF that was grown on the conductive electrode surface.[87] This compound showed a CO_2/CO overpotential of ~650 mV, Faraday efficiency of ~100%, TOF of 0.13 s^{-1}, and TON of 1520, and all of these values are superior to those of the corresponding homometallic catalysts.

While the aforementioned two reports did not show a cooperative effect due to the presence of multi- and heterometal ions, a report by Beobide *et al.* demonstrated that Zn^{II}–Cu^{II}, Ru^{III}–Cu^{II}, and Pd^{II}–Cu^{II} MOFs that were prepared by post-synthesis transmetallation of HKUST-1(Cu) containing benzene-1,3,5-tricarboxylate (BTC) exhibit a heterometallic effect.[88] The sample solid was dispersed in a Nafion–isopropanol solution and drop-cast on an electrode to be applied for electrocatalytic CO_2 reduction. Although the amount of transmetallated metal ions was less than 19%, the CO_2 reduction catalytic activity was strikingly increased by this heterometal doping. In particular, the selective formation of EtOH reached 100%.

In 2020, Dong and Feng *et al.* reported 2D sheet Cu^{II}–Zn^{II} MOFs with phthalocyanine ligands, which showed the synergistic electroreduction of carbon dioxide (Fig. 5).[89] The solid sample was prepared by the self-assembly method under solvothermal conditions and loaded on an electrode together with a mixture of carbon nanotubes and Nafion. These conjugated 2D sheet MOFs revealed excellent catalytic performance with a CO product selectivity of 88%, TOF of 0.39 s^{-1}, and durability of >10 hours. Notably, this material showed that the molar H_2/CO ratio was reduced from 4 : 1 to 1 : 7 when the metal centres and applied potentials were varied. Cu^{II} ions coordinated by phthalocyanine-N4 in a square-planar geometry and Zn^{II} ions coordinated by two catecholato units in a square-planar geometry were assigned as the active centres for hydrogen evolution and CO production, respectively. The Cu^{II} and Zn^{II} centres synergistically inhibited H_2 production and promoted CO production *via* electrons that passed through π-conjugated ligands. Examples of MOFs that show electrocatalytic CO_2 reduction have been summarized in a recent review article.[90]

6. O_2 reduction electrocatalysis

Oxygen reduction is an important chemical reaction in the design of fuel cell devices and metal–air batteries.[91] The best catalyst for oxygen reduction is platinum metal containing carbon (Pt/C), but platinum is expensive and scarce.[92] Therefore, non-precious alternative catalysts for oxygen reduction are in high demand, especially those that meet the requirements of large-scale commercial applications. One of the major studies related to alternative catalysts is the use of composite materials derived from CPs or MOFs.[93] However, their preparation requires energy-consuming pyrolysis/calcination under harsh synthesis conditions, which results in the destruction of their original ordered structures and a loss of active sites.[94] The use of CPs for oxygen reduction reactions is still at an early research phase, having started only in 2012,[95] and studies using heterometallic CPs have rarely been reported.[96–100] The Dehghanpour group reported that a Zr-MOF with Zr_6^{IV} oxo-clusters linked by Fe^{III} porphyrins acted as an oxygen reduction catalyst.[96] The Zr^{IV}–Fe^{III} MOF was further mixed with pyridine-functionalized graphene and then drop-cast on a glassy carbon electrode. The modified electrode revealed enhanced catalytic activity for oxygen reduction in cyclic voltammograms with a maximum current that was 61.6 times larger than that of the bare electrode. In addition, this

Table 2 Structural and electrocatalytic parameters for pristine O_2 evolution electrocatalysts based on their heterometallic coordination polymers

Compound	Dimension	Metal	Organic ligand/metalloligand	Onset potential	η	TOF	Tafel slope	Electrolyte	Ref.
$K_{2x}Co_{(2-x)}[Fe(CN)_6]$ ($0.85 < x < 0.95$)	3D	Co^{II} and Fe^{III}	CN^-	+1.10 V (*vs.* NHE)	400 mV (@ 1 mA cm^{-2})	2×10^{-3} s^{-1} (η = 300 mV) and 0.5 s^{-1} (η = 550 mV)	85–95 mV dec^{-1}	pH 7 KP_i (50 mM) + 1 M KNO_3	76
$K_aCo_b[Fe(CN)_6]\cdot xH_2O$	3D	Co^{II} and Fe^{II}	CN^-	—	692 mV (@ 1 mA cm^{-2})	3.0×10^{-3} s^{-1} (η = 400 mV)	121 mV dec^{-1}	pH 7 KP_i (50 mM) + 1 M KNO_3	77
$K_aCo_b[Fe(CN)_6]\cdot xH_2O$	3D	Co^{II} and Fe^{III}	CN^-	—	661 mV (@ 1 mA cm^{-2})	4.4×10^{-3} s^{-1} (η = 400 mV)	127 mV dec^{-1}	pH 7 KP_i (50 mM) + 1 M KNO_3	77
$K_aCo_b[Cr(CN)_6]\cdot xH_2O$	3D	Co^{II} and Cr^{III}	CN^-	—	578 mV (@ 1 mA cm^{-2})	5.0×10^{-3} s^{-1} (η = 400 mV)	96 mV dec^{-1}	pH 7 KP_i (50 mM) + 1 M KNO_3	77
[$CoFe(CN)_6$@FTO]	3D	Co^{II} and Fe^{II}	CN^-	—	600 mV (@ 1 mA cm^{-2})	2.6×10^{-3} s^{-1} (η = 262 mV)	111 mV dec^{-1}	pH 7 KP_i (50 mM) + 1 M KNO_3	78
[$CoFe(CN)_6$-PVP@FTO]	3D	Co^{II} and Fe^{II}	CN^-	—	510 mV (@ 1 mA cm^{-2})	2.6×10^{-3} s^{-1} (η = 284 mV)	121 mV dec^{-1}	pH 7 KP_i (50 mM) + 1 M KNO_3	78
$Fe_{0.5}Ni_{0.5}$Pc-CP	2D	Fe^{II} and Ni^{II}	(2(3),9(10),16(17),23(24)-Tetraiodophthalocyanine and 2(3),9(10),16(17),23(24)-tetra(ethynyl)phthalocyanine)	—	317 mV (@ 10 mA cm^{-2})	43.4 s^{-1} (η = 317 mV)	116 mV dec^{-1}	1.0 M KOH	79
[$ZnCl(H_2O)Cu_2Pt_2(NH_3)_4$(D-pen)$_4$]Cl	1D	Cu^{II}, Pt^{II} and Zn^{II}	D-Penicillaminate (D-pen)	+0.75 V (*vs.* Ag/AgCl)	133 mV	18 h^{-1}	—	0.1 K KPF_6	80
[$ZnCu_2Pt_2(NH_3)_4$(D-pen)$_4$]$(ClO_4)_2$	3D	Cu^{II}, Pt^{II} and Zn^{II}	D-Penicillaminate (D-pen)	+0.75 V (*vs.* Ag/AgCl)	133 mV	27 h^{-1}	—	0.1 K KPF_6	80
MOF									
Fe/Ni_x-MIL-53 (x = 1.6, 2.0, 2.4)	2D	Fe^{III} and Ni^{II}	1,4-Bezenedicarboxylate (1,4-BDC)	—	258, 258 and 244 mV (@ 10 mA cm^{-2})	—	37.8, 45.5 and 48.7 mV dec^{-1}	1.0 M KOH	82
Fe/$Ni_{2.4}$/M_x-MIL-53 (M = Co, Mn; x = 0.2, 0.4)	2D	Fe^{III}, Ni^{II} and M^{II}	1,4-Bezenedicarboxylate (1,5-BDC)	—	219 mV (@ 10 mA cm^{-2})	—	53.5 mV dec^{-1}	1.0 M KOH	82
$Ni_{0.8}Fe_{0.2}(C_{12}H_6O_4)(H_2O)_4$	3D	Fe^{III} and Ni^{II}	2,6-Naphthalenedicarboxylic acid	—	240 mV (@ 10 mA cm^{-2})	3.8 s^{-1} (η = 400 mV)	34 mV dec^{-1}	0.1 M KOH	83

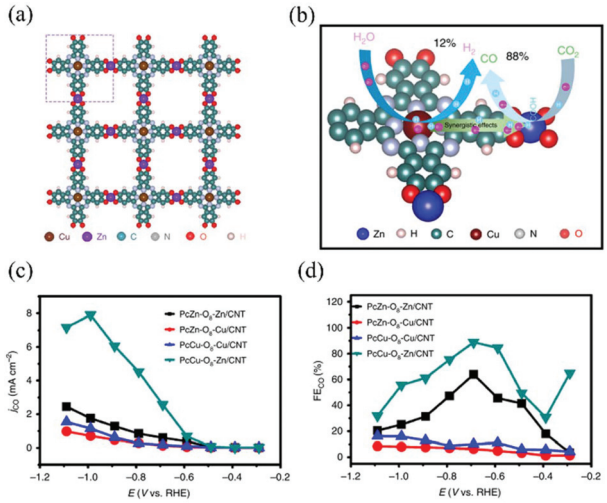

Fig. 5 Cu^{II}–Zn^{II} bimetallic coordination polymers as a CO_2 reduction electrocatalyst: (a) packing structure, (b) a proposed synergistic catalytic scheme based on DFT calculations, (c) partial current and (d) Faraday efficiency of CO production at different potentials. Adapted from ref. 89.

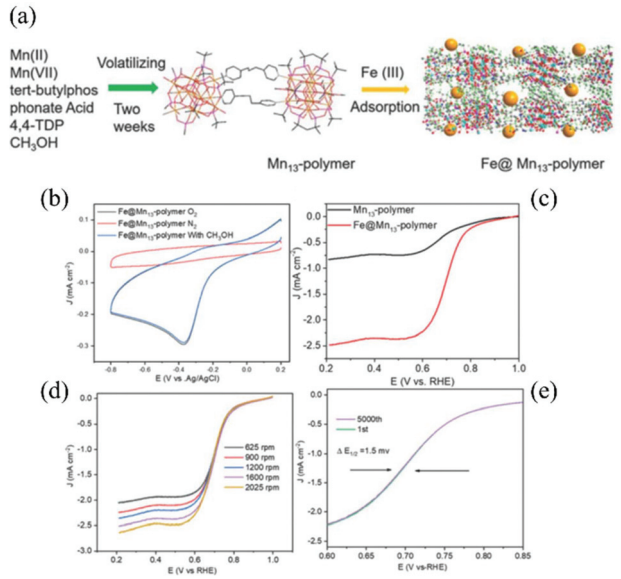

Fig. 6 Fe^{III}–Mn^{II} bimetallic coordination polymers as an O_2 reduction electrocatalyst: (a) synthesis scheme and structures, (b) CV curves in 1.0 M CH_3OH containing a N_2- and O_2-saturated 0.1 M solution of KOH at a scan rate of 0.1 V s^{-1}, (c) LSV curves at a scan rate of 0.01 V s^{-1}, (d) oxygen reduction polarization curves at different rotation rates, and (e) oxygen reduction polarization curves before and after 5000 potential cycles. Adapted from ref. 99 with permission from The Royal Society of Chemistry.

MOF system showed improved stability and repeatability. They suggested that the 3D MOF structure prevented the aggregation of the active units of the Fe^{III} porphyrin, contrasting the case of conventional discrete molecular systems. The Morris group also studied the catalytic behaviour of the same Zr^{IV}–Fe^{III} MOF.[97] They directly grew a MOF film on a FTO electrode by a solvothermal method without using graphene. The thin film of the heterometallic Zr^{IV}–Fe^{III} MOF had enough conductivity to perform catalytic oxygen reduction without any conductive additives. Electrochemical characterization revealed high selectivity for H_2O ($4e^-$ reduction product) over H_2O_2 ($2e^-$ reduction product) with this material.

Jiang and Yao *et al.* reported an ethyl-linked Fe^{III}/Co^{II} polymer conjugated with phthalocyanine that acted as a heterogeneous oxygen reduction catalyst.[98] The conjugated polymers were synthesized by a Sonogashira coupling reaction between Fe^{III} and Co^{II} phthalocyanine monomers in Fe : Co ratios of 100 : 0, 50 : 50, and 0 : 100. The homo- and heterometallic polymers were loaded on glassy carbon electrodes with 50% carbon black (Vulcan XC-72), and their catalytic activities for oxygen reduction were evaluated by CV, LSV, and rotating ring-disk electrode (RRDE) measurements. The heterometallic conjugated polymer revealed a catalytic activity superior to that of the corresponding homometallic polymers, indicating a synergistic effect between the Fe^{III} and Co^{II} centres that were located in close proximity to each other in the heterometallic polymer.

Zhang *et al.* employed a Mn^{II}_{13} coordination polymer containing Fe^{III} ions as an oxygen reduction catalyst (Fig. 6).[99] They expected that the Fe^{III} ions dispersed into the coordination polymer would show catalytic activity, although Fe^{III} ions tend to form an aggregate that is catalytically inactive. The Fe^{III} ions were introduced by immersing freshly prepared crystals of the porous Mn^{II}_{13} coordination polymer with *tert*-butylphosphonate and 4,4′-trimethylenedipyridine in an aqueous solution of $FeCl_3$. The obtained microcrystals were characterized by RRDE and LSV measurements using a glassy carbon electrode loaded with a sample-Nafion mixture. While the Mn^{II}_{13} coordination polymer itself exhibited a catalytic current during oxygen reduction, as observed by LSV, the doped Fe^{III} ions led to an improved onset potential and a smaller Tafel slope (130 mV dec^{-1}), indicative of a synergistic effect due to the Fe^{III} and Mn^{II} centres. Furthermore, this heterometallic coordination polymer was highly tolerant towards methanol, which is a typical fuel crossover.

In general, catalytic oxygen reduction reactions require a low overpotential, high kinetics (Tafel slope, TOF and TON), high selectivity (H_2O *vs.* H_2O_2 *vs.* H_2) and high stability. Thus, heterometallic CPs are promising materials for these catalytic reactions due to their robust framework and the synergistic and cooperative effects of their heterometal ions.[100] While their low conductivities may be a weak point, this issue has now been overcome by the use of redox-active frameworks or the inclusion of conductive species in the framework. Further development of heterometallic CPs as oxygen reduction electrocatalysts will have a significant impact on this research field.

7. Organic reaction electrocatalysis

Heterometallic CPs have also been studied for the catalytic activation of small organic molecules such as alcohols, organic

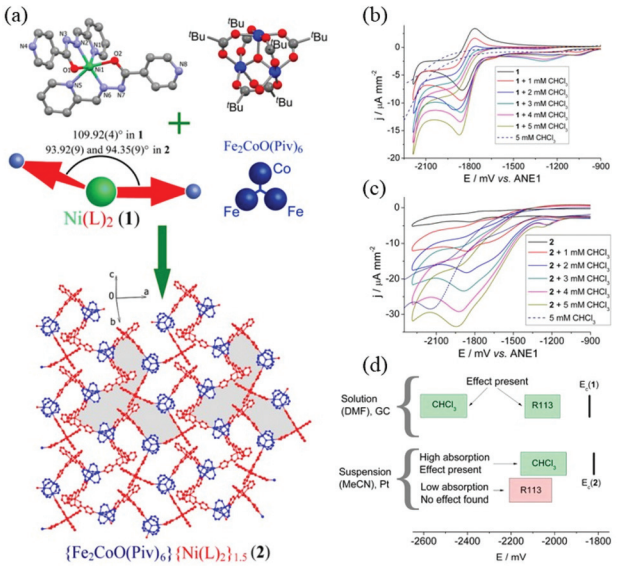

Fig. 7 A Fe^{III}–Ni^{II} bimetallic coordination polymer as a dehalogenation electrocatalyst: (a) synthesis scheme and structures, (b) CV curves of the Ni^{II} metalloligand in DMF with the addition of $CHCl_3$, (c) CV curves of the suspension containing the Fe^{III}–Ni^{II} bimetallic coordination polymer in CH_3CN with the addition of $CHCl_3$, and (d) catalytic activities *vs.* redox potentials of the catalysts and the halides. Adapted with permission from ref. 102, Copyright 2014 American Chemical Society.

acids, and organic halides.[101] The Kolotilov group reported the electrocatalytic dehalogenation of organic halides using a Fe^{III}–Co^{II}–Ni^{II} heterotrimetallic CP (Fig. 7).[102] They prepared a mononuclear nickel(II) complex with a Schiff base ligand that was derived from the hydrazine of 4-pyridinecarboxylic acid and 2-pyridinecarbaldehyde to act as a N-donating metalloligand. By mixing this nickel(II) metalloligand with the trigonal trinuclear cluster, $[Fe_2CoO(piv)_6]$, which consists of Co^{II} and Fe^{III} ions bridged by pivalate (piv) ligands, the Fe^{III}–Co^{II}–Ni^{II} heterotrimetallic CP was isolated as a crystalline solid. The nickel(II) metalloligand is a ligand-based redox-active species that shows two reduction processes in homogeneous cyclic voltammograms. The first reduction current increased with the addition of $CHCl_3$, indicating that the nickel(II) metalloligand itself had electrocatalytic activity for the dehalogenation of organic halides. Thus, this group showed that the Fe^{III}–Co^{II}–Ni^{II} heterotrimetallic CP functioned as a heterogeneous electrocatalyst for the dehalogenation of organic halides due to the presence of the nickel(II) metalloligand.

Since electrocatalytic current is commonly much higher than the current of a standard redox process, it is often used as the signal for molecular sensors working in solution.[103] Furthermore, the electrocatalytic response is specific for substrates, which is also an advantage for the design of selective and sensitive molecular sensors. Ma and Pang *et al.* reported a 3d–4f heterometallic MOF compound that consisted of Mn^{II}–W^{VI} Dawson-type POM units linked by Ce^{III} species with *N*-oxide bipyridine ligands.[104] The Mn^{II}–W^{VI}–Ce^{III} MOF was prepared by a reaction of Mn^{II}–W^{VI} POM with Ce^{III} species. Cyclic voltammetry using a sample-modified carbon paste electrode showed that the oxidation peak currents for the Mn^{II} and Ce^{III} centres substantially increased with the addition of either ascorbic acid or dopamine. This result indicated that the oxidations of ascorbic acid and dopamine were catalysed by the Mn^{II}–W^{VI}–Ce^{III} MOF. On the other hand, this current increase was not observed for the Mn^{II}–W^{VI} POM. The Ma group established another detection system using a heterometallic CP.[105] They prepared a film of a cyano-bridged heterometallic CP containing poly(L-citrulline)/lanthanide on a glassy carbon electrode, and it was applied for the electrochemical detection of 3-nitropropionic acid. A linear relationship between the peak currents due to reduction of 3-nitropropionic acid and the 3-nitropropionic acid concentration was obtained for the range of 40.0–4.00 × 10^3 μM. Wang *et al.* conducted the electrocatalytic oxidation of ethanol using a Nd–Fe–Mo cyano-bridged CP.[106] The fabrication of this coordination polymer on a platinum electrode was performed by electrochemical deposition. While platinum atoms on the electrode surface were assigned to catalytic reaction centres, the heterometallic CP provided a cooperative effect reconstructing the environment around the platinum surface, improving the ethanol oxidation kinetics.

In the past decade, an increasing number of studies have been devoted to heterometallic CPs as promising heterogeneous catalysts for a variety of organic reactions, such as the cyanosilylation of aldehydes,[107] oxidation of cyclohexene,[108] olefin epoxidation,[109] the Knoevenagel condensation,[110] cyanation of aldehydes,[111] sulfoxidation,[112] imine formation from alcohols and amines,[113] regioselective halogenation of phenol,[114] hydrogenation,[115] desulfurization,[116] the Henry reaction,[117] C–S cross-coupling reactions,[118] organophosphate hydrolysis,[119] oxidative hydroxylation of phenylboronic acid,[120] nitroaldol reactions,[121] acetalization of benzaldehyde,[122] and reduction of nitrophenol.[123] The above catalytic reactions often involve redox reactions using chemical reagents (*i.e.*, H_2O_2, O_2, and $NaBH_4$), and their corresponding electrocatalytic reactions have not been reported to date. This observation is most likely due to the difficulty in the fabrication/loading of CPs on electrodes, which requires tight and close contact between the electrode and sample. Furthermore, the complexity of analysing electrochemical responses due to organic species using voltammograms prevents the development and expansion of this research field. Further trials are needed to elucidate the mechanisms of heterogeneous, electrocatalytic organic transformations, in which synergistic effects are expected due to the different kinds of metal centres existing in heterometallic CPs.

8. Summary and perspectives

While CPs have been applied to obtain inorganic composite materials by their pyrolysis in materials science, recently, an increasing number of studies have been conducted on their direct employment as heterogeneous electrocatalysts because they are (i) crystalline compounds whose molecular and

packing structures can be determined at an atomic-level resolution by X-ray crystallography, (ii) solid materials that can offer high stability in the solid state, and (iii) hybrid compounds that contain metal ions available for catalytically active sites. The tunability of the active sites in the structure, such as the oxidation states and the coordination geometries of metal ions and the distances between metal centres, is also the reason for the recent interest from researchers. In particular, heterogeneous electrocatalytic reactions using heterometallic CPs containing more than two kinds of metal ions, which can be prepared by the self-assembly of metal ions and ligands in a one-pot reaction, the metalloligand approach using metal complexes with several donor sites, or the post-synthesis modification of CPs by metal exchange reactions, are a recent hot topic in this research area, because their metal centres cause synergistic and cooperative effects in electrocatalytic reactions. Therefore, these CPs can lead to enhanced electrocatalytic performances, which are highly expected for this class of compounds. To date, hydrogen evolution (water/proton reduction), oxygen evolution (water oxidation), oxygen reduction, carbon dioxide reduction, and organic transformation have been studied as heterogeneous electrocatalytic reactions using CPs, all of which depend on the differences in the geometries and oxidation states of metal ions incorporated in the CPs.

Porous coordination polymers (PCPs) with MOFs are a major class of heterometallic CPs, and they have been a target of study for their effects on heterogeneous electrocatalytic activity. This is because porous structures allow the insertion and accommodation of catalytically active and electrically conductive species, electrolytes, substrates, and solvents, which can overcome the weakness of CPs in various applications. While the best performance of heterogeneous electrocatalytic activity has been achieved by conductive MOFs, some non-porous CPs have also shown electrocatalytic activities due to the addition of external species, such as Nafion and carbon materials, which serve as binders and electrical conductors, respectively. As part of studies on heterogeneous electrocatalysis, methods for sample loading on electrodes, such as crystal growth, electrodeposition, and transcription, have also been developed by applied chemists.[47]

The electronic communication between the catalytically active centres of metal ions can enhance not only the electrical conductivity but also the synergistic effects, leading to a higher performance during electrocatalytic reactions. In coordination chemistry, it is quite important to determine the best combinations of metal ions that lead to the enhancement in electrocatalytic activity and to elucidate enhancement mechanisms. As described in this review article, the favourable combinations of metal ions in CPs appear to be dependent on the type of electrocatalytic reaction, and the design of metal combinations that cause high activities relies on the large number of screening experiments based on reported heterometallic systems. The insufficient number of reports on the heterogeneous electrocatalytic activities of heterometallic CPs and the lack of theoretical studies make it difficult to predict their synergistic effects on electrocatalytic activities. Thus, fundamental studies focused on investigating the relationships between structures and catalytic activities and the synthesis of new heterometallic CPs with unique molecular and crystal structures are highly desired, although arguments exist regarding whether the original polymeric structures are fully retained in the course of electrocatalytic reactions.

Most reports on heterogeneous electrocatalysis using heterometallic CPs have appeared only in recent decades. In this research field, the discovery of new heterometallic CPs that show excellent electrocatalytic activities should be promising *via* cooperative studies on coordination chemistry, catalytic chemistry, and electrochemistry.

Conflicts of interest

There are no conflicts to declare.

Acknowledgements

This work was supported by JSPS KAKENHI (grant numbers 18H05344 and 19K05667).

Notes and references

1 S. R. Batten, N. R. Champness, X.-M. Chen, J. Garcia-Martinez, S. Kitagawa, L. Öhrström, M. O'Keeffe, M. P. Suh and J. Reedijk, Coordination polymers, metal–organic frameworks and the need for terminology guidelines, *CrystEngComm*, 2012, **14**, 3001–3004.
2 J. C. Bailaer Jr., Coordination Polymers, *Prep. Inorg. React.*, 1964, 1.
3 J.-Q. Liu, Z.-D. Luo, Y. Pan, A. K. Singh, M. Trivedi and A. Kumar, Recent developments in luminescent coordination polymers: Designing strategies, sensing application and theoretical evidences, *Coord. Chem. Rev.*, 2020, **406**, 213145.
4 X. Zhang, W. Wang, Z. Hu, G. Wang and K. Uvdal, Coordination polymers for energy transfer: Preparations, properties, sensing applications, and perspectives, *Coord. Chem. Rev.*, 2015, **284**, 206–235.
5 B. Chen, S. Xiang and G. Qian, Metal–Organic Frameworks with Functional Pores for Recognition of Small Molecules, *Acc. Chem. Res.*, 2010, **43**, 1115–1124.
6 M. L. Foo, R. Tatsuda and S. Kitagawa, Functional Hybrid Porous Coordination Polymers, *Chem. Mater.*, 2014, **26**, 310–322.
7 D. Maspoch, D. Ruiz-Molina and J. Veciana, Magnetic nanoporous coordination polymers, *J. Mater. Chem.*, 2004, **14**, 2713–2723.
8 Y.-Z. Zheng, Z. Zheng and X.-M. Chen, A symbol approach for classification of molecule-based magnetic materials exemplified by coordination polymers of metal carboxylates, *Coord. Chem. Rev.*, 2014, **258–259**, 1–15.

9 T. Uemura, N. Yanai and S. Kitagawa, Polymerization reactions in porous coordination polymers, *Chem. Soc. Rev.*, 2009, **38**, 1228–1236.
10 E. Loukopoulos and G. E. Kostakis, Review: Recent advances of one-dimensional coordination polymers as catalysts, *J. Coord. Chem.*, 2018, **71**, 371–410.
11 F. A. Aldeida, P. J. Klinowski, S. M. F. Vilela, J. P. C. Tome, J. A. S. Cavaleiro and J. Rocha, Ligand design for functional metal–organic frameworks, *Chem. Soc. Rev.*, 2012, **41**, 1088–1110.
12 N. Li, R. Feng, J. Zhu, Z. Chang and X.-H. Bu, Conformation versatility of ligands in coordination polymers: From structural diversity to properties and applications, *Coord. Chem. Rev.*, 2018, **375**, 558–586.
13 M. Andruh, Heterotrimetallic complexes in molecular magnetism, *Chem. Commun.*, 2018, **54**, 3559–3577.
14 W.-H. Zhang, Q. Liu and J.-P. Lang, Heterometallic transition metal clusters and cluster-supported coordination polymers derived from Tp- and Tp*-based Mo(W) sulfido precursors, *Coord. Chem. Rev.*, 2015, **293–294**, 187–210.
15 M. Andruh, J.-P. Costes, C. Diaz and S. Gao, 3d-4f Combined Chemistry: Synthetic Strategies and Magnetic Properties, *Inorg. Chem.*, 2009, **48**, 3342–3359.
16 S. Zhang and P. Cheng, Recent advances in the construction of lanthanide–copper heterometallic metal–organic frameworks, *CrystEngComm*, 2015, **17**, 4250–4271.
17 C. L. Cahill, D. T. de Lill and M. Frisch, Homo- and heterometallic coordination polymers from the f elements, *CrystEngComm*, 2007, **9**, 15–26.
18 S. Chorazy, M. Wyczesany and B. Sieklucka, Lanthanide Photoluminescence in Heterometallic Polycyanidometallate-Based Coordination Networks, *Molecules*, 2017, **22**, 1902.
19 T. A. Goetjen, J. Liu, Y. Wu, J. Sui, X. Zhang, J. T. Hupp and O. M. Farha, Metal–organic framework (MOF) materials as polymerization catalysts: a review and recent advances, *Chem. Commun.*, 2020, **56**, 10409–10418.
20 P.-Q. Liao, J.-Q. Shen and J.-P. Zhang, Metal–organic frameworks for electrocatalysis, *Coord. Chem. Rev.*, 2018, **73**, 22–48.
21 Q. Wang and D. Astruc, State of the Art and Prospects in Metal–Organic Framework (MOF)-Based and MOF-Derived Nanocatalysis, *Chem. Rev.*, 2020, **120**, 1438–1511.
22 K. Biradha, A. Goswami and R. Moi, Coordination polymers as heterogeneous catalysts in hydrogen evolution and oxygen evolution reactions, *Chem. Commun.*, 2020, **56**, 10824–10842.
23 H. Zhang, J. Su, K. Zhao and L. Chen, Recent Advances in Metal-Organic Frameworks and Their Derived Materials for Electrocatalytic Water Splitting, *ChemElectroChem*, 2020, **7**, 1805–1824.
24 W. Wang, X. Xu, W. Zhou and Z. Shao, Recent Progress in Metal-Organic Frameworks for Applications in Electrocatalytic and Photocatalytic Water Splitting, *Adv. Sci.*, 2017, **4**, 1600371.
25 L. Qin and H.-G. Zhang, Structures and applications of metal–organic frameworks featuring metal clusters, *CrystEngComm*, 2017, **19**, 745–757.
26 G. Kumar and R. Gupta, Molecularly designed architectures—the metalloligand way, *Chem. Soc. Rev.*, 2013, **42**, 9403–9453.
27 S. Mukhopadhyay, O. Basu, R. Nasani and S. K. Das, Evolution of metal organic frameworks as electrocatalysts for water oxidation, *Chem. Commun.*, 2020, **56**, 11735–11748.
28 Y. H. Budnikova, Recent advances in metal-organic frameworks for electrocatalytic hydrogen evolution and overall water splitting reactions, *Dalton Trans.*, 2020, **49**, 12483–12502.
29 F. Zheng, Z. Zhang, C. Zhang and W. Chen, Advanced Electrocatalysts Based on Metal-Organic Frameworks, *ACS Omega*, 2020, **5**, 2495–2502.
30 D. Zhu, M. Qiao, J. Liu, T. Tao and C. Guo, Engineering pristine 2D metal-organic framework nanosheets for electrocatalysis, *J. Mater. Chem. A*, 2020, **8**, 8143–8170.
31 J.-Y. Zue, C. Li, F. Long, H.-W. Gu, P. Braunstein and J.-P. Lang, Recent advances in pristine metal-organic frameworks toward the oxygen evolution reaction, *Nanoscale*, 2020, **12**, 4816–4825.
32 B. A. Friese and D. G. Kurth, From coordination complex to coordination polymers through self-assembly, *Curr. Opin. Colloid Interface Sci.*, 2009, **14**, 81–93.
33 J. Gil-Rubio and J. Vicente, The Coordination and Supramolecular Chemistry of Gold Metalloligands, *Chem. – Eur. J.*, 2018, **24**, 32–46.
34 W.-X. Zhang, P.-Q. Liao, R.-B. Lin, Y.-S. Wei, M.-H. Zeng and X.-M. Chen, Metal cluster-based functional porous coordination polymers, *Coord. Chem. Rev.*, 2015, **293–294**, 263–278.
35 A. Y. Robin and K. M. Fromm, Coordination polymer networks with O- and N-donors: What they are, why and how they are made, *Coord. Chem. Rev.*, 2006, **259**, 2127–2157.
36 T. D. Bennett and S. Horike, Liquid, glass and amorphous solid states of coordination polymers and metal–organic frameworks, *Nat. Rev. Mater.*, 2018, **3**, 431–440.
37 S. Srivastava and R. Gupta, Metalloligands to material: design strategies and network topologies, *CrystEngComm*, 2016, **48**, 9185–9208.
38 T. Matsumoto, H.-C. Chang, A. Kobayashi, K. Uosaki and M. Kato, Metal-Dependent and Redox-Selective Coordination Behaviors of Metalloligand $[Mo^{V}(1,2\text{-benzenedithiolato})_3]^-$ with Cu^{I}/Ag^{I} Ions, *Inorg. Chem.*, 2011, **50**, 2859–2869.
39 Z. Ying, S. Wan, J. Yang, M. Kurmoo and M. H. Zeng, Recent Advances in Post-Synthetic Modification of Metal-Organic Frameworks: New Types and Tandem Reactions, *Coord. Chem. Rev.*, 2019, **378**, 500.
40 M. Lalonde, W. Bury, O. Karagiaridi, Z. Brown, J. T. Hupp and O. K. Farha, Transmetalation: route to metal exchange within metal-organic frameworks, *J. Mater. Chem. A*, 2013, **1**, 5453–5468.

41 J. Lee, O. K. Farha, J. Roberts, K. A. Scheidt, S. T. Nguyen and J. T. Hupp, Metal-organic framework materials as catalysts, *Chem. Soc. Rev.*, 2009, **38**, 1450–1459.
42 M. Fang and B. Zhao, Ln-Ag heterometallic coordination polymers, *Rev. Inorg. Chem.*, 2015, **35**, 81–113.
43 G. Givaja, P. Amo-Ochoa, C. J. Gómez-García and F. Zamora, Electrical conductive coordination polymers, *Chem. Soc. Rev.*, 2012, **41**, 115–147.
44 S. Liu, A. Motta, A. R. Mouat, M. Delferro and T. J. Marks, Very Large Cooperative Effects in Heterobimetallic Titanium-Chromium Catalysts for Ethylene Polymerization/Copolymerization, *J. Am. Chem. Soc.*, 2014, **136**, 10460–10469.
45 A. Deronzier and J.-C. Moutet, Polypyrrole films containing metal complexes: syntheses and applications, *Coord. Chem. Rev.*, 1996, **147**, 339–371.
46 A. Doménech-Carbó, J. Labuda and F. Scholz, Electroanalytical chemistry for the analysis of solids: Characterization and classification (IUPAC Technical Report), *Pure Appl. Chem.*, 2013, **85**, 609–631.
47 Y.-H. Xiao, Z.-G. Gu and J. Zhang, Surface-coordinated metal – organic framework thin films (SURMOFs) for electrocatalytic applications, *Nanoscale*, 2020, **12**, 12712–12730.
48 K. Zeng and D. Zhang, Recent progress in alkaline water electrolysis for hydrogen production and applications, *Prog. Energy Combust. Sci.*, 2010, **36**, 307–326.
49 M. Drosou, F. Kamatsos and C. A. Mitsopoulou, Recent advances in the mechanisms of the hydrogen evolution reaction by non-innocent sulphur-coordinating metal complexes, *Inorg. Chem. Front.*, 2020, **7**, 37–71.
50 T. Abe, F. Taguchi, S. Tokita and M. Kaneko, Prussian White as a highly active molecular catalyst for proton reduction, *J. Mol. Catal. A: Chem.*, 1997, **126**, L89–L92.
51 E. P. Alsac, E. Ulker, S. V. K. Nune and F. Karadas, A Cyanide-Based Coordination Polymer for Hydrogen Evolution Electrocatalysis, *Catal. Lett.*, 2018, **148**, 531–538.
52 M. Nihei, Molecular Prussian Blue Analogues: From Bulk to Molecules and Low-dimensional Aggregates, *Chem. Lett.*, 2020, **49**, 1206–1215.
53 T. Abe, G. Toda, A. Tajiri and M. Kaneko, Electrochemistry of ferric ruthenocyanide (Ruthenium Purple), and its electrocatalysis for proton reduction, *J. Electroanal. Chem.*, 2001, **510**, 35–42.
54 T. Abe, N. Kawai, A. Tajiri and M. Kaneko, Electrochemistry of Ruthenium Purple Confined in a Polymer Matrix: Voltammetry, Electrocatalysis for Hydrogen Evolution, and ElectronTransport Characteristics, *Bull. Chem. Soc. Jpn.*, 2003, **76**, 645–650.
55 A. Ghaffarinejad, N. Sadeghi, H. Kazemi, A. Khajehzadeh, M. Amiri and A. Noori, Effect of metal hexacyanoferrate films on hydrogen evolution reaction, *J. Electroanal. Chem.*, 2012, **685**, 103–108.
56 B. Keita and L. Nadjo, Activation of electrode surfaces: Application to the lectrocatalysis of the hydrogen evolution reaction, *J. Electroanal. Chem.*, 1985, **191**, 441–448.
57 J.-W. Zhao, Y.-Z. Li, L.-J. Chen and G.-Y. Yand, Research progress on polyoxometalate-based transition-metal–rare-earth heterometallic derived materials: synthetic strategies, structural overview and functional applications, *Chem. Commun.*, 2016, **52**, 4418–4445.
58 B. Keita, U. Kortz, L. R. B. Holze, S. Brown and L. Nadjo, Efficient Hydrogen-Evolving Cathodes Based on Proton and Electron Reservoir Behaviors of the Phosphotungstate $[H_7P_8W_{48}O_{184}]^{33-}$ and the Co(II)-Containing Silicotungstates $[Co_6(H_2O)_{30}\{Co_9Cl_2(OH)_3(H_2O)_9(\beta\text{-}SiW_8O_{31})_3\}]^{5-}$ and $[\{Co_3(B\text{-}\beta\text{-}SiW_9O_{33}(OH))(B\text{-}\beta\text{-}SiW_8O_{29}OH)_2\}_2]^{22-}$, *Langmuir*, 2007, **23**, 9531–9534.
59 J.-S. Qin, D.-Y. Du, W. Guan, X.-J. Bo, Y.-F. Li, L.-P. Guo, Z.-M. Su, Y.-Y. Wang, Y.-Q. Lan and H.-C. Zhou, Ultrastable Polymolybdate-Based Metal–Organic Frameworks as Highly Active Electrocatalysts for Hydrogen Generation from Water, *J. Am. Chem. Soc.*, 2015, **137**, 7169–7177.
60 L. Zhang, S. Li, C. J. Gómez-García, H. Ma, C. Zhang, H. Pang and B. Li, Two Novel Polyoxometalate-Encapsulated Metal–Organic Nanotube Frameworks as Stable and Highly Efficient Electrocatalysts for Hydrogen Evolution Reaction, *ACS Appl. Mater. Interfaces*, 2018, **10**, 31498–31504.
61 J. Cai, X. Y. Zheng, J. Xie, Z.-H. Yan, X.-J. Kong, Y.-P. Ren, L.-S. Long and L.-S. Zheng, Anion-Dependent Assembly of Heterometallic 3d–4f Clusters Based on a Lacunary Polyoxometalate, *Inorg. Chem.*, 2017, **56**, 8439–8445.
62 W. Salomon, G. Paille, M. Gomez-Mingot, P. Mialane, J. Marrot, C. Roch-Marchal, G. Nocton, C. Mellot-Draznieks, M. Fontecave and A. Dolbecq, Effect of Cations on the Structure and Electrocatalytic Response of Polyoxometalate-Based Coordination Polymers, *Cryst. Growth Des.*, 2017, **17**, 1600–1609.
63 N. Yoshinari and T. Konno, Chiral Phenomena in Multinuclear and Metallosupramolecular Coordination Systems Derived from Metalloligands with Thiol-containing Amino Acids, *Bull. Chem. Soc. Jpn.*, 2018, **91**, 790–812.
64 N. Yoshinari and T. Konno, Metallosupramolecular Structures Derived from a Series of Diphosphine-bridged Digold(I) Metalloligands with Terminal D-Penicillamine, *Chem. Rec.*, 2016, **16**, 1647–1663.
65 A. Igashira-Kamiyama and T. Konno, Rational creation of chiral multinuclear and metallosupramolecular compounds from thiol-containing amino acids, *Dalton Trans.*, 2011, **40**, 7249–7263.
66 N. Kuwamura, Y. Kurioka and T. Konno, A platinum(II)-palladium(II)-nickel(II) heterotrimetallic coordination polymer showing a cooperative effect on catalytic hydrogen evolution, *Chem. Commun.*, 2017, **53**, 846–849.
67 Y. Kurioka, N. Kuwamura, N. Yoshinari, A. Igashira-Kamiyama and T. Konno, A New Platinum(II) Metalloligand System with D-Penicillaminate: An Excellent Stereoselectivity in the Formation of S-bridged $Pt^{II}_2CoIII_2$ and $Pt^{II}_2NiII_2$ Complexes with Opposite

Hydrogen-bonding Helix Structures, *Chem. Lett.*, 2015, **44**, 1330–1332.

68 A. C. San Esteban, N. Kuwamura, T. Kojima and T. Konno, Dimensional Structures and Electrocatalytic Activities of Platinum(II)-Palladium(II)-Manganese(II) Coordination Polymers Controlled by Chloride versus Bromide, *Inorg. Chem.*, 2020, **59**, 14847–14851.

69 R. Shekurov, V. Khrizanforova, L. Gilmanova, M. Khrizanforov, V. Miluykov, O. Kataeva, Z. Yamakeeva, T. Burganov, T. Gerasimova, A. Khamargalimov, S. Katsyuba, V. Kovalenko, Y. Krupskaya, V. Kataev, B. Büchner, V. Bon, I. Senkobska, S. Kaskel, A. Gubaidullin, O. Sinyashin and Y. Budnikova, Zn and Co redox active coordination polymers as efficient electrocatalysts, *Dalton Trans.*, 2019, **48**, 3601–3609.

70 V. Khrizanforova, R. Shekurov, V. Miluykov, M. Khrizanforov, V. Bon, S. Kaskel, A. Gubaidullin, O. Sinyashin and Y. Budnikova, 3D Ni and Co redox-active metal–organic frameworks based on ferrocenyl diphosphinate and 4,4′-bipyridine ligands as efficient electrocatalysts for the hydrogen evolution reaction, *Dalton Trans.*, 2020, **49**, 2794–2802.

71 H. Huang, Y. Zhao, Y. Bai, F. Li, Y. Zhang and Y. Chen, Conductive Metal–Organic Frameworks with Extra Metallic Sites as an Efficient Electrocatalyst for the Hydrogen Evolution Reaction, *Adv. Sci.*, 2020, **7**, 2000012.

72 H. Noh, C.-W. Kung, K. Otake, A. W. Peters, Z. Li, Y. Liao, X. Gong, O. K. Farha and J. T. Hupp, Redox-Mediator-Assisted Electrocatalytic Hydrogen Evolution from Water by a Molybdenum Sulfide-Functionalized Metal–Organic Framework, *ACS Catal.*, 2018, **8**, 9848–9858.

73 M. D. Kärkäs and B. Äkermark, Water oxidation using earth-abundant transition metal catalysts: opportunities and challenges, *Dalton Trans.*, 2016, **45**, 14421–14461.

74 D. W. Shaffer, Y. Xie and J. J. Concepcion, O–O bond formation in ruthenium-catalyzed water oxidation: single-site nucleophilic attack *vs.*, O–O radical coupling, *Chem. Soc. Rev.*, 2017, **46**, 6170–6193.

75 M. A. Asraf, H. A. Younus, M. Yusubovc and F. Verpoort, Earth-abundant metal complexes as catalysts for water oxidation; is it homogeneous or heterogeneous?, *Catal. Sci. Technol.*, 2015, **5**, 4901–4925.

76 S. Pintado, S. Goberna-Ferrón, E. C. Escudero-Adán and J. R. Galán-Mascarós, Fast and Persistent Electrocatalytic Water Oxidation by Co–Fe Prussian Blue Coordination Polymers, *J. Am. Chem. Soc.*, 2013, **135**, 13270–13273.

77 E. P. Alsaç, E. Ülker, S. V. K. Nune, Y. Dede and F. Karadas, Tuning the Electronic Properties of Prussian Blue Analogues for Efficient Water Oxidation Electrocatalysis: Experimental and Computational Studies, *Chem. – Eur. J.*, 2018, **24**, 4856–4863.

78 M. Aksoy, S. V. K. Nune and F. Karadas, A Novel Synthetic Route for the Preparation of an Amorphous Co/Fe, Prussian Blue Coordination Compound with High Electrocatalytic, Water Oxidation Activity, *Inorg. Chem.*, 2018, **55**, 4301–4307.

79 D. Qi, X. Chen, W. Liu, C. Liu, W. Liu, K. Wang and J. Jiang, A Ni/Fe-based heterometallic phthalocyanine conjugated polymer for the oxygen evolution reaction, *Inorg. Chem. Front.*, 2020, **7**, 642–646.

80 N. Kuwamura, Y. Kurioka, N. Yoshinari and T. Konno, Heterogeneous Catalytic Water Oxidation Controlled by Coordination Geometries of Copper(II) Centers with Thiolato Donors, *Chem. Commun.*, 2018, **54**, 10766–10769.

81 D. Yang, Y. Chen, Z. Su, X. Zhang, W. Zhang and K. Srinivas, Organic carboxylate-based MOFs and derivatives for electrocatalytic water oxidation, *Coord. Chem. Rev.*, 2021, **428**, 213619.

82 X.-L. Wang, L.-Z. Dong, M. Qiao, Y.-J. Tang, J. Liu, T. Li, S.-L. Li, J.-X. Su and Y.-Q. Lan, Exploring the Performance Improvement of the Oxygen Evolution Reaction in a Stable Bimetal-Organic Framework System, *Angew. Chem., Int. Ed.*, 2018, **5**, 9660–9664.

83 J. Duan, S. Chen and C. Zhao, Ultrathin metal-organic framework array for efficient electrocatalytic water splitting, *Nat. Commun.*, 2017, **8**, 15341.

84 M. Aresta, A. Dibenedetto and A. Angelini, Catalysis for the Valorization of Exhaust Carbon: from CO_2 to Chemicals, Materials, and Fuels. Technological Use of CO_2, *Chem. Rev.*, 2014, **114**, 1709–1742.

85 R. Hinogami, S. Yotsuhashi, M. Deguchi, Y. Zenitani, H. Hashiba and Y. Yamada, Electrochemical Reduction of Carbon Dioxide Using a Copper Rubeanate Metal Organic Framework, *ECS Electrochem. Lett.*, 2012, **1**, H17–H19.

86 N. Kornienko, Y. Zhao, C. S. Kley, C. Zhu, D. Kim, S. Lin, C. J. Chang, O. M. Yaghi and P. Yang, Metal–Organic Frameworks for Electrocatalytic Reduction of Carbon Dioxide, *J. Am. Chem. Soc.*, 2015, **137**, 14129–14135.

87 I. Hod, M. D. Sampson, P. Deria, C. P. Kubiak, O. K. Farha and J. T. Hupp, Fe-Porphyrin-Based Metal–Organic Framework Films as High-Surface Concentration, Heterogeneous Catalysts for Electrochemical Reduction of CO_2, *ACS Catal.*, 2015, **5**, 6302–6309.

88 M. Perfecto-Irigaray, J. Albo, G. Beobide, O. Castilloa, A. Irabienb and S. Pérez-Yáñez, Synthesis of heterometallic metal–organic frameworks and their performance as electrocatalyst for CO_2 reduction, *RSC Adv.*, 2018, **8**, 21092–21099.

89 H. Zhong, M. Ghorbani-Asl, K. H. Ly, J. Zhang, J. M. Wang, Z. Liao, D. Makarov, E. Zschech, E. Brunner, I. M. Weidinger, J. Zhang, A. V. Krasheninnikov, S. Kakel, R. Dong and X. Feng, Synergistic electroreduction of carbon dioxide to carbon monoxide on bimetallic layered conjugated metal-organic frameworks, *Nat. Commun.*, 2020, **11**, 1409.

90 F. N. Al-Rowaili, A. Jamal, M. S. Ba Shammakh and A. Rana, A Review on Recent Advances for Electrochemical Reduction of Carbon Dioxide to Methanol Using Metal–Organic Framework (MOF) and Non-MOF Catalysts: Challenges and Future Prospects, *ACS Sustainable Chem. Eng.*, 2018, **6**, 15895–15914.

91 M. Kefevre, R. Proietti, F. Jaouen and J.-P. Dodelet, Iron-Based Catalysts with Improved Oxygen Reduction Activity in Polymer Electrolyte Fuel Cells, *Science*, 2009, **324**, 71–74.

92 T. Yu, D. Y. Kim, H. Zhang and Y. Xia, Platinum concave nanocubes with high-index facets and their enhanced activity for oxygen reduction reaction, *Angew. Chem., Int. Ed.*, 2011, **50**, 2773–2777.

93 G. Wu, K. L. More, C. M. Johnston and P. Zelenay, High-Performance Electrocatalysts for Oxygen Reduction Derived from Polyaniline, Iron, and Cobalt, *Science*, 2011, **332**, 443–447.

94 J. Wang, Z. Huang, W. Liu, C. Chang, H. Tang, Z. Li, W. Chen, C. Jia, T. Yao, S. Wei, Y. Wu and Y. Li, Design of N-Coordinated Dual-Metal Sites: A Stable and Active Pt-Free Catalyst for Acidic Oxygen Reduction Reaction, *J. Am. Chem. Soc.*, 2017, **139**, 17281–17284.

95 M. Jahan, Q. Bao and K. P. Loh, Electrocatalytically Active Graphene–Porphyrin MOF Composite for Oxygen Reduction Reaction, *J. Am. Chem. Soc.*, 2012, **134**, 6707–6713.

96 S. Sohrabi, S. Dehghanpour and M. Ghalkhani, Three-Dimensional Metal–Organic Framework Graphene, Nanocomposite as a Highly Efficient and Stable, Electrocatalyst for the Oxygen Reduction Reaction in, Acidic Media, *ChemCatChem*, 2016, **8**, 2356–2366.

97 P. M. Usov, B. Huffman, C. C. Epley, M. C. Kessinger, J. Zhu, W. A. Maza and A. J. Morris, Study of Electrocatalytic Properties of Metal-Organic Framework PCN-223 for the Oxygen Reduction Reaction, *ACS Appl. Mater. Interfaces*, 2017, **9**, 33539–33543.

98 W. Liu, Y. Hou, H. Pan, W. Liu, D. Qi, K. Wang, J. Jiang and X. Yao, An ethynyl-linked Fe/Co heterometallic phthalocyanine conjugated polymer for the oxygen reduction reaction, *J. Mater. Chem. A*, 2018, **6**, 8349–8357.

99 T. Wen, W. Schmitt and L. Zhang, An Fe(III)-doped coordination polymer of Mn_{13}-clusters with improved activity of the oxygen reduction reaction, *Dalton Trans.*, 2019, **48**, 4794–4797.

100 H. Yoon, S. Lee, S. Oh, H. Park, S. Choi and M. Oh, Synthesis of Bimetallic Conductive 2D Metal–Organic Framework (Co_xNi_y-CAT) and Its Mass Production: Enhanced Electrochemical Oxygen Reduction Activity, *Small*, 2019, **15**, 1805232.

101 X. Feng, C. Xu, Z.-Q. Wang, S.-F. Tang, W.-J. Fu, B.-M. Ji and L.-Y. Wang, Aerobic Oxidation of Alcohols and the Synthesis of Benzoxyazoles Catalyzed by Cuprocupric Coordination Polymer (Cu^+-CP) Assisted by TEMPO, *Inorg. Chem.*, 2015, **54**, 2088–2090.

102 A. S. Lytvynenko, S. V. Kolotilov, M. A. Kiskin, O. Cador, S. Golhen, G. G. Aleksandrov, A. M. Mishura, V. E. Titov, L. Ouahab, I. L. Eremenko and V. M. Novotortsev, Redox-Active Porous Coordination Polymers Prepared by Trinuclear, Heterometallic Pivalate Linking with the Redox-Active Nickel(II), Complex: Synthesis, Structure, Magnetic and Redox Properties, and, Electrocatalytic Activity in Organic Compound Dehalogenation in, Heterogeneous Medium, *Inorg. Chem.*, 2014, **53**, 4970–4979.

103 B. S. Sherigara, W. Kutner and F. D'Souza, Electrocatalytic Properties and Sensor Applications of Fullerenes and Carbon Nanotubes, *Electroanalysis*, 2003, **15**, 753–772.

104 T. Yu, H. Ma, C. Zhang, H. Pang, S. Li and H. Liu, A 3d-4f heterometallic 3D POMOF on lacunary Dawson polyoxometalates, *Dalton Trans.*, 2013, **42**, 16328–16333.

105 S. Wang, M. Zhou, Y. Zhu, B. Peng, J. Yang and Y. Ma, Voltammetric Detection of 3-Nitropropionic Acid in Sugarcane Juices Using a Poly(L-citrulline)/Lanthanide-Containing Cyano-Bridged Heterometallic Coordination Polymer Modified Electrode, *J. Electrochem. Soc.*, 2020, **167**, 086508.

106 Y. Ma, Y. Du, W. Ye, B. Su, M. Yang and C. Wang, Electrocatlytic Oxidation of Ethanol on Platinum Electrode Decorated with Nd-Fe-Mo Hybride-metallic Cyano-Bridged Mixing Coordination Polymer in Weak Acid Medium, *Int. J. Electrochem. Sci.*, 2012, **7**, 2654–2679.

107 J.-J. Du, X. Zhang, X.-P. Zhou and D. Li, Robust heterometallic MOF catalysts for the cyanosilylation of aldehydes, *Inorg. Chem. Front.*, 2018, **5**, 2772–2776.

108 D. Sun, F. Sun, X. Deng and Z. Li, Mixed-Metal Strategy on Metal-Organic Frameworks (MOFs) for Functionalities Expansion: Co Substitution Induces Aerobic Oxidation of Cyclohexene over Inactive Ni-MOF-74, *Inorg. Chem.*, 2015, **54**, 8639–8643.

109 G. Kumar, G. Kumar and R. Gupta, Manganese- and Cobalt-Based Coordination Networks as Promising Heterogeneous Catalysts for Olefin Epoxidation Reactions, *Inorg. Chem.*, 2015, **54**, 2603–2615.

110 L.-J. Yue, Y.-Y. Liu, G.-H. Xu and J.-F. Ma, Calix[4]arene-based polyorometalate organic-inorganic hybrid and coronation polymer as heterogeneous catalysts for azide-alkyne cycloaddition and Knoevenagel condensation reaction, *New J. Chem.*, 2019, **43**, 15871–15878.

111 D. Bansal, S. Pandey, G. Hudal and R. Gupta, Heterometallic coordination polymers: syntheses, structures and heterogeneous catalytic applications, *New J. Chem.*, 2015, **39**, 9772–9781.

112 M. Yadav, A. Bhunia, S. K. Jana and P. W. Roesky, Manganese- and Lanthanide-Based 1D Chiral Coordination Polymers as an Enantioselective Catalyst for Sulfoxidation, *Inorg. Chem.*, 2016, **55**, 2701–2708.

113 G.-J. Chen, H.-C. Ma, W.-L. Xin, X.-B. Li, F.-Z. Jin, J.-S. Wang, M.-Y. Liu and Y.-B. Dong, Dual Heterogeneous Catalyst Pd-Au@Mn(II)-MOF for One-pot Tandem Synthesis of Imines from Alcohols and Amines, *Inorg. Chem.*, 2017, **56**, 654–660.

114 C. Huang, K. Zhu, Y. Zhang, Z. Shao, D. Wang, L. Mi and H. Hou, Directed Structural Transformations of Coordination Polymers Supported Single-Site Cu(II) Catalysts To Control the Site Selectivity of C–H Halogenation, *Inorg. Chem.*, 2019, **58**, 12933–12942.

115 L. Yu, Z. Wang, J. Wu, S. Tu and K. Ding, Directed Orthogonal Self-Assembly of Homochiral Coordination Polymes for Heterogeneous Enantioselective Hydrogenetion, *Angew. Chem., Int. Ed.*, 2010, **49**, 3627–3630.

116 Y.-Y. Ma, H.-Q. Tan, Y.-H. Wang, X.-L. Hao, X.-J. Feng, H.-Y. Zang and Y.-G. Li, *CrystEngComm*, 2015, **17**, 7938–7947.

117 M. Gupta, D. De, S. Pal, T. K. Pal and K. Tomar, A porous two-dimensional Zn(II)-coordination polymer exhibiting SC-SC transmetalation with Cu(II): efficient heterogeneous catalysis for the Henry reaction and detection of nitro explosives, *Dalton Trans.*, 2017, **46**, 7619–7627.

118 G. Kumar, F. Hussain and R. Gupta, Carbon-sulphur cross coupling reactions catalyzed by nickel-based coordination polymers based on metalloligands, *Dalton Trans.*, 2017, **46**, 15023–15031.

119 H. Tabe, M. Matsushima, R. Tanaka and Y. Yamada, Creation and stabilization of tunable open metal sites in thiocyanato-bridged heterometallic coordination polymers to be used as heterogeneous catalysts, *Dalton Trans.*, 2019, **48**, 17063–17069.

120 S. J. Bora, R. Paul, A. Dutta, S. Goswami, A. J. Guha and A. J. Thakur, Trinuclear Mn^{2+}/Zn^{2+} based microporous coordination polymers as efficient catalysts for *ipso*-hydroxylation of boronic acids, *Dalton Trans.*, 2020, **49**, 5454–5462.

121 A. K. Jana and S. Natarajan, Cu_6S_6 Clusters as a Building Block for the Stabilization of Coordination Polymers with NiAs, NaCl, and Related Structures: Synthesis, Structure, and Catalytic Studies, *Eur. J. Inorg. Chem.*, 2018, 739–750.

122 A. Dikhtiarenko, S. A. Khainakov, I. de Pedro, J. A. Blanco, J. García and J. Gimeno, Series of 2D Heterometallic Coordination Polymers Based on Ruthenium(III) Oxalate Building Units: Synthesis, Structure, and Catalytic and Magnetic Properties, *Inorg. Chem.*, 2013, **52**, 3933–3941.

123 S. A. Sotnik, R. A. Polunin, M. A. Kiskin, A. M. Kirillov, V. N. Dorofeeva, K. S. Gavrilenko, I. L. Eremenko, V. M. Novotortsev and S. V. Kolotilov, Heterometallic Coordination Polymers Assembled from Trigonal Trinuclear Fe_2Ni-Pivalate Blocks and Polypyridine Spacers: Topological Diversity, Sorption, and Catalytic Properties, *Inorg. Chem.*, 2015, **54**, 5169–5181.